# Effect of Diluents on Membrane Formation via Thermally Induced Phase Separation

HIDETO MATSUYAMA,[1] MASAAKI TERAMOTO,[1] SHUNSUKE KUDARI,[2] YOSHIRO KITAMURA[2]

[1] Department of Chemistry and Materials Technology, Kyoto Institute of Technology, Matsugasaki, Sakyo-ku, Kyoto 606-8585, Japan

[2] Department of Environmental Chemistry and Materials, Okayama University, 2-1-1 Tsushima-naka, Okayama 700-8530, Japan

*Received 12 May 2000; accepted 6 October 2000*

**ABSTRACT:** The effect of diluents on isotactic polypropylene (iPP) membrane formation via thermally induced phase separation was investigated. The diluents were methyl salicylate (MS), diphenyl ether (DPE), and diphenylmethane (DPM). The cloud-point curve was shifted to a lower temperature in the order iPP–MS, iPP–DPE, and iPP–DPM, whereas the crystallization temperature was not influenced so much by diluent type. Droplet-growth processes were investigated under two conditions: quenching the polymer solution at the desired temperature and cooling at a constant rate. Although droplet sizes were in the order iPP–MS, iPP–DPE, and iPP–DPM in both cases, the difference was more pronounced with the constant cooling rate condition. Scanning electron microscopy indicated that interconnected structures were obtained when the polymer solution was quenched in ice water. The effect of the diluents on these structures was observed. © 2001 John Wiley & Sons, Inc. J Appl Polym Sci 82: 169–177, 2001

**Key words:** thermally induced phase separation; effect of diluent; polypropylene

## INTRODUCTION

Thermally induced phase separation (TIPS) is one of the major techniques for the preparation of polymeric porous membranes by controlled phase separation.[1–11] TIPS is mainly classified into two types: solid–liquid (S–L) TIPS, in which the polymer crystallizes out of solution, and liquid–liquid (L–L) TIPS, in which the solution separates into a polymer-rich matrix phase and a polymer-lean droplet phase. A typical phase diagram is shown in Figure 1 for when these two processes occur sequentially. In the TIPS process, a polymer is dissolved in a diluent at a high temperature. With the cooling of the solution, L–L phase separation is induced when the solution goes inside the binodal line. When a crystallization temperature is reached, S–L phase separation (polymer crystallization) occurs, and the structure is fixed. Then, the diluent is removed by extraction, evaporation, or freeze drying, and a porous membrane is obtained.

In the TIPS process, how the diluent should be selected is an important problem for controlling the pore size. The compatibility of polymer and diluent directly reflects thermodynamic properties such as the binodal line and crystallization temperature. As the compatibility becomes lower, the binodal line is shifted to a higher temperature,[7] as shown by the arrow in Figure 1, whereas the crystallization temperature is less influenced

*Correspondence to:* H. Matsuyama (matuyama@chem.kit.ac.jp).

Journal of Applied Polymer Science, Vol. 82, 169–177 (2001)

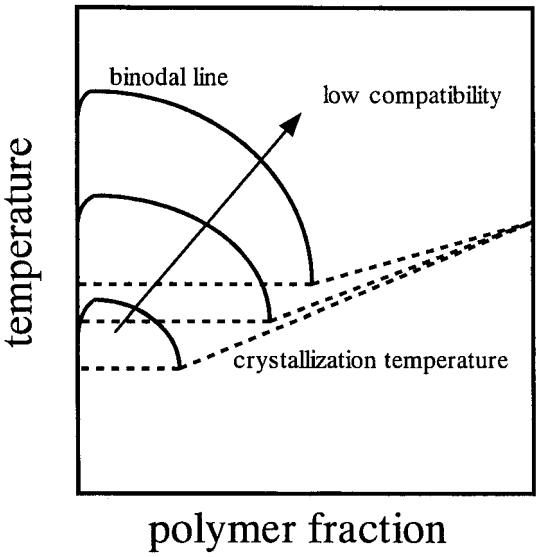


**Figure 1** Typical phase diagram in TIPS process.

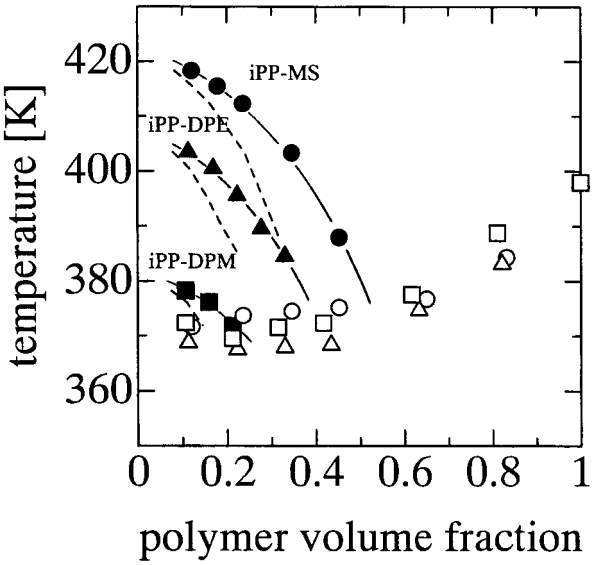


**Figure 2** Phase diagrams for the three polymer–diluent systems: cloud points for (●) iPP–MS, (▲) iPP–DPE, and (■) iPP–DPM and crystallization temperatures for (○) iPP–MS, (△) iPP–DPE, and (□) iPP–DPM. Dotted lines are the calculated spinodal lines.

by the compatibility. This means that the region between the binodal line and the crystallization temperature becomes wider in the case of low compatibility, which results in a longer time for pore growth in the cooling process. Furthermore, when the position of the binodal line changes, kinetic properties such as the phase-separation rate and pore-growth rate may be changed because these rates are functions of the temperature and composition of phase-separated solutions.

Lee et al.[12] investigated the relation between L–L phase separation and crystallization by applying a systematic change in the interaction in polypropylene–diluent systems. A series of dialkyl phthalates with a different number of carbon atoms in the alkyl chain was used as the diluent. The L–L phase-separation temperature decreased remarkably when the number of carbon atoms in the diluents increased, whereas the melting-point curve remained constant. However, they did not report the effect of diluents on the kinetic properties of the pore-growth rate and so on. The phase behaviors of a ternary mixture of diluent–diluent–polyethylene were investigated by Vadalia et al.[13] to control systematically L–L phase separation and crystallization by changing the composition of two diluents. They showed that a ternary solution could be considered a pseudobinary polymer solution with various diluent qualities. Kinetic properties were also beyond their interest.

In this work, the effect of diluents on polypropylene membrane formation was investigated with three kinds of diluents. The droplet-growth rates in three systems were investigated and discussed on the basis of the phase diagram.

## EXPERIMENTAL

### Materials

The polymer was isotactic polypropylene (iPP; Aldrich Chemical Co.; weight-average molecular weight = 250,000). Methyl salicylate (MS), diphenyl ether (DPE), and diphenylmethane (DPM) were used as diluents without further purification. These diluents were purchased from Nacalai Tesque Co. (Kyoto, Japan).

**Table I Solubility Parameters**

| Substance | Solubility Parameter ($MPa^{1/2}$) |
|---|---|
| Polypropylene | 18.8[a] |
| MS | 21.7[a] |
| DPE | 20.7[b] |
| DPM | 19.5[b] |

[a] Reference 15.
[b] Reference 16.

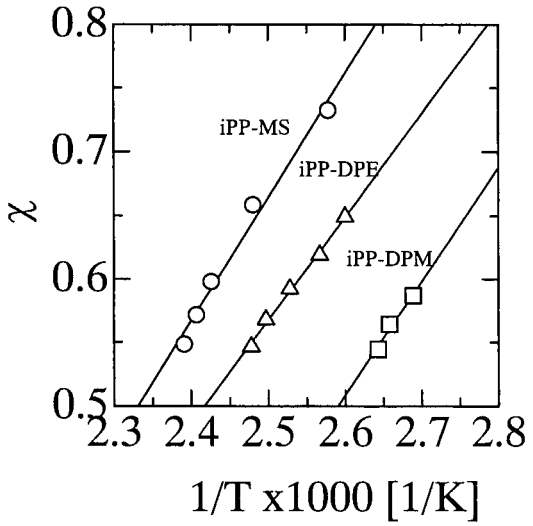


**Figure 3** Relation between $\chi$ and $1/T$.

### Phase Diagram

A homogeneous solid polymer–diluent sample was prepared with a method previously described.[8] The solid sample was chopped into small pieces and placed between a pair of microscope coverslips. To prevent diluent loss by evaporation, we inserted a Teflon film 100 $\mu$m thick with a square opening in the center between the coverslips. The coverslip sample was heated on a hot stage (Linkam LK-600PH) at 443 K for 1 min and then cooled at a controlled rate of 10 or 100 K/min with a Linkam L-600A controller. We determined cloud points visually by noting the appearance of turbidity under a microscope (Olympus BX50, Tokyo, Japan).

Differential scanning calorimetry (DSC; Perkin-Elmer DSC-7) was used to determine the crystallization temperature for the dynamic phase diagram. The solid polymer–diluent sample was sealed in an aluminum DSC pan, melted at 473 K for 5 min, and then cooled at 10 K/min to 298 K. The onset of the exothermic peak during the cooling was taken as the crystallization temperature.

### Droplet-Growth Measurement

The hot stage was placed on the platform of the optical microscope. Droplet-growth processes

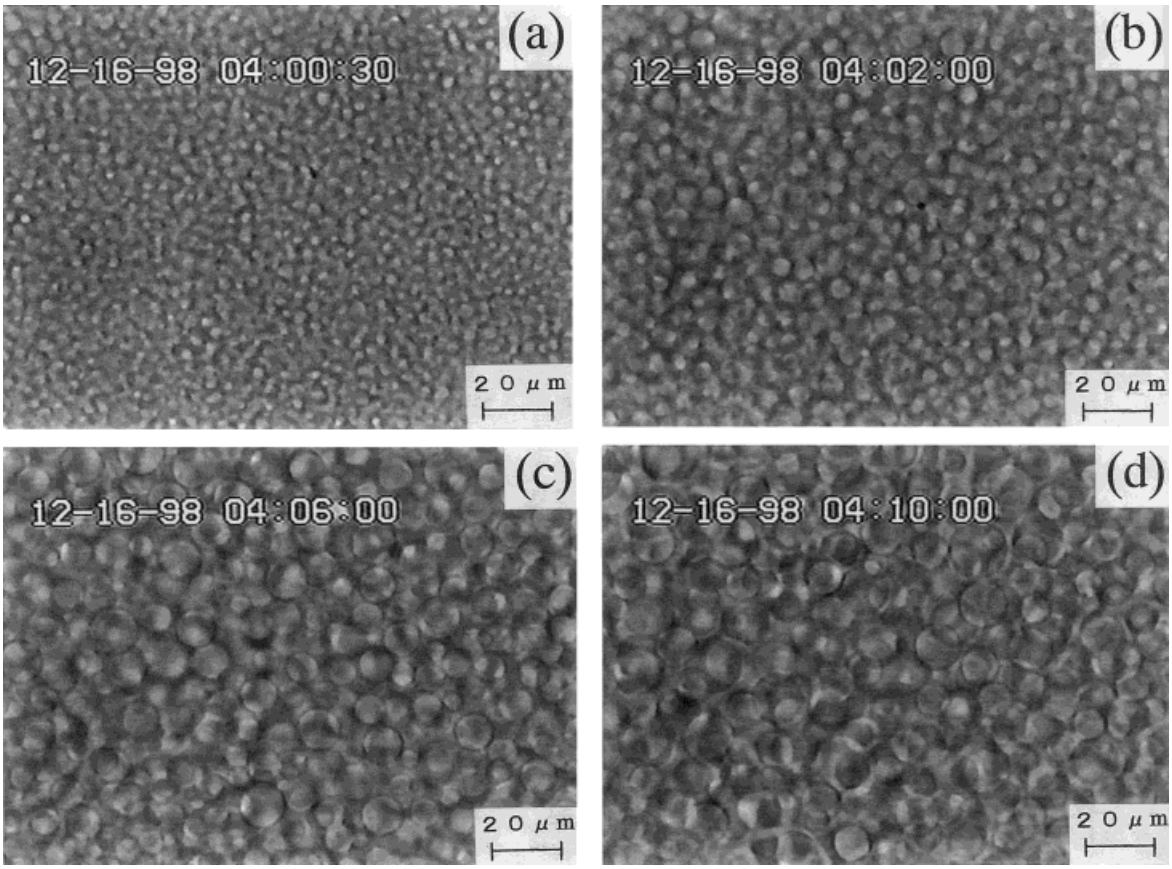


**Figure 4** Optical micrographs of droplets formed in the iPP–MS system at 415.3 K with a polymer concentration of 10 wt %: (a) 0.5, (b) 2.0, (c) 6.0, and (d) 10.0 min.

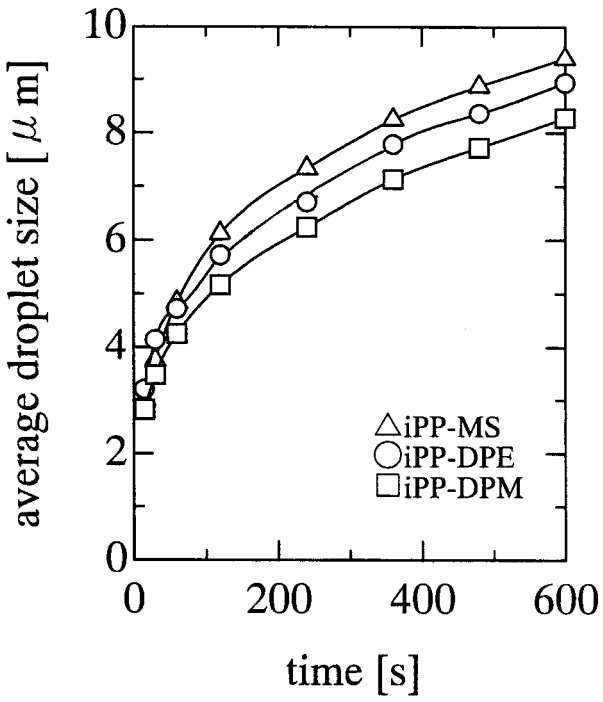


**Figure 5** Time course of the average droplet size with a polymer concentration of 10 wt %. In the three systems, the temperatures at which the polymer solutions were quenched were 3.0 K lower than the cloud-point temperatures.

were investigated under two conditions: quenching the polymer solution at a desired temperature and cooling at a constant rate. The sample sealed with two coverslips was placed on the stage and heated at a temperature 10 K higher than the cloud point for 5 min. Then, it was quenched to the desired temperature at a cooling rate of 130 K/min or cooled to 298 K at the constant cooling rates of 10 and 100 K/min. The image from the microscope was converted into a video signal. To obtain the average droplet size of the polymer-lean phase, we used image analysis. The image analysis software package was Win ROOF (Mitani Co., Fukui, Japan).

### Measurement of Polymer-Rich Phase Viscosity

Viscosity was measured with a falling-sphere viscometer.[14] A homogeneous solid polymer–diluent sample was heated in a glass bottle at 443 K to cause melt blending. Then, the polymer solution was poured into a glass cylinder with a radius of $5.03 \times 10^{-3}$ m, and the cylinder was immersed in an oil bath with the temperature controlled at the desired value. A stainless steel sphere with a radius of $3.18 \times 10^{-3}$ m was dropped, and the time necessary to move the constant length was measured. The relation between the viscosity and falling time is available in the literature.[14]

### Scanning Electron Microscopy (SEM) Observations

In the sample cooled at the controlled rate, the diluent was extracted with methanol, and the methanol was evaporated to produce the microporous membrane. The same treatment was done for the sample quenched immediately in the ice water after the sample was heated on the hot stage to cause melt blending. The microporous membrane was fractured in liquid nitrogen and mounted vertically on a sample holder. The sample of the membrane was sputtered with Au/Pd *in vacuo*. A scanning electron microscope (Hitachi Co. S-2150, Tokyo, Japan) with an accelerating voltage of 15 kV was used to examine the membrane cross sections.

## RESULTS AND DISCUSSION

### Phase Diagram

Figure 2 shows the phase diagrams in three polymer–diluent systems. The iPP–MS system showed the highest cloud-point curve. In the order of iPP–MS, iPP–DPE, and iPP–DPM, the cloud-point curve was shifted to the lower temperature, whereas the crystallization temperature was not influenced so much by the diluent

**Table II Volume Fraction of the Droplet Phase, Interfacial Tension, and Matrix Phase Viscosity**

| System | Volume Fraction of the Droplet Phase | Interfacial Tension (mN/m) | Matrix Phase Viscosity (Pa s) |
|---|---|---|---|
| iPP–MS | 0.37 | 0.021 | 1.2 |
| iPP–DPE | 0.31 | 0.011 | 1.8 |
| iPP–DPM | 0.38 | 0.014 | 5.4 |

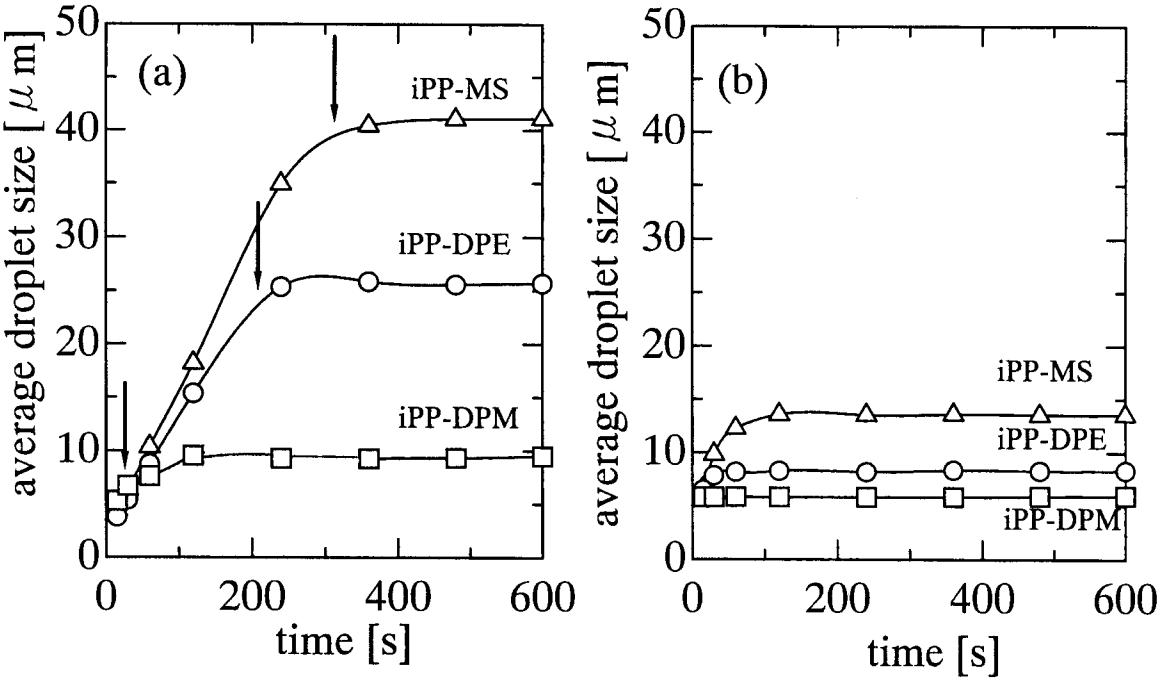


**Figure 6** Droplet growth under nonisothermal conditions with cooling rates of (a) 10 and (b) 100 K/min with a polymer concentration of 10 wt %.

type. This weak effect of the diluents on the crystallization temperature agrees with results reported previously.[12,13] The solubility parameters for iPP, MS, DPE, and DPM are summarized in Table I. The difference in the solubility parameters between iPP and MS is largest and decreases in the order iPP–MS, iPP–DPE, and iPP–DPM. This means that the compatibility increases in this order. Because the high compatibility brings about the decrease of the cloud-point curve, the tendency in the cloud points can be explained by the change in the compatibility.

Equating polymer chemical potentials in two phase-separated phases based on the Flory–Huggins theory[17] gives the following two equations describing the binodal line:[18]

$$\{(\phi_2^\beta)^2 - (\phi_2^\alpha)^2\}\chi = \ln\left(\frac{1-\phi_2^\alpha}{1-\phi_2^\beta}\right) + \left(1 - \frac{1}{r}\right)(\phi_2^\alpha - \phi_2^\beta) \quad (1)$$

$$r\{(1-\phi_2^\beta)^2 - (1-\phi_2^\alpha)^2\}\chi = \ln\left(\frac{\phi_2^\alpha}{\phi_2^\beta}\right) + (r-1)(\phi_2^\alpha - \phi_2^\beta) \quad (2)$$

where $\phi_2^\alpha$ and $\phi_2^\beta$ are the polymer volume fractions in the polymer-rich and polymer-lean phases, respectively; $\chi$ is the interaction parameter; and $r$ is the ratio of the polymer molar volume to the diluent molar volume. As a first approximation, the cloud points were assumed to be representative of the coexistence curve.[18] With $\phi_2^\alpha$ shown in Figure 2 and eqs. (1) and (2), $\chi$ at each temperature $T$ was estimated. Figure 3 shows the relation of $\chi$ and $1/T$. Straight lines were obtained in all three cases. Flory's theory gives the following equation for spinodal lines:

$$\frac{1}{\nu_1(1-\phi_2)} + \frac{1}{\nu_2\phi_2} - \frac{2\chi}{\nu_1} = 0 \quad (3)$$

where $\nu$ is the molar volume and the subscripts 1 and 2 denote diluent and polymer, respectively. The spinodal lines calculated from eq. (3) with $\chi$ parameters from Figure 3 are shown in Figure 2 as dotted lines.

## Droplet-Growth Process

Figure 4 shows examples of optical micrographs of droplets formed in the iPP–MS system. Droplet size clearly increased as time proceeded. The time course of the average droplet size, which was obtained by image analysis of the optical micrograph,

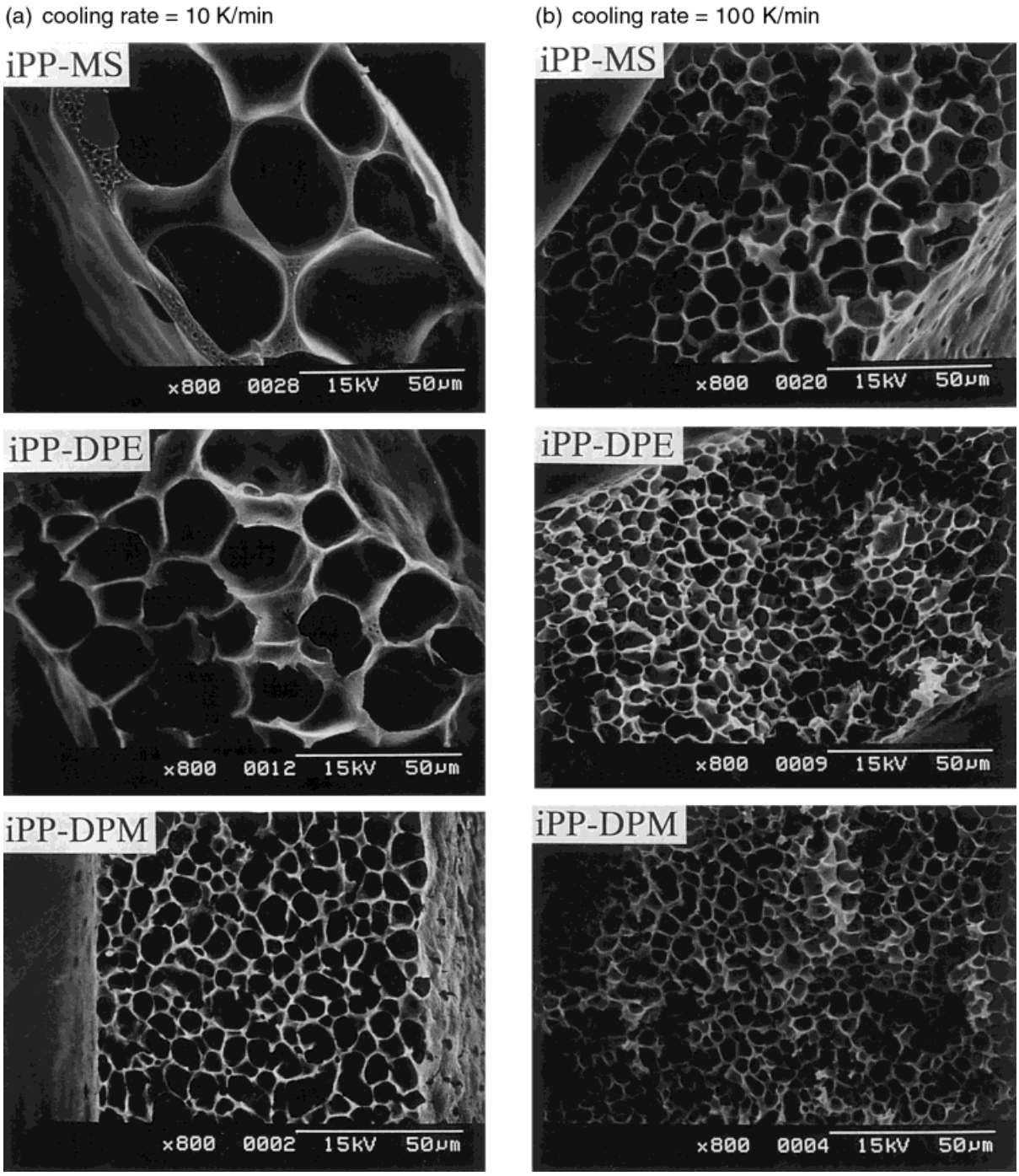


**Figure 7** Cross sections of membranes prepared by cooling at 10 K/min and 100 K/min with a polymer concentration of 10 wt %.

is shown in Figure 5. In this experiment, the polymer solution was quenched to the desired temperature, and the temperature was maintained. In three systems, temperatures at which the polymer solution was quenched were 3.0 K lower than the respective cloud-point temperatures. The quench depths from the calculated spinodal temperatures were about 1.5 K and were almost the same in the three cases. The initial droplet sizes were almost identical for the three systems. As time proceeds, a difference in the droplet sizes with the diluent type became more pronounced. The iPP–MS system

**Table III Comparison Between Pore Size and Droplet Size**

| Cooling Rate (K/min) | System | Pore Size ($\mu$m) | Droplet Size ($\mu$m) | Pore Size/Droplet Size |
|---|---|---|---|---|
| 10 | iPP–MS | 35.3 | 41.0 | 0.86 |
| | iPP–DPE | 19.6 | 25.7 | 0.76 |
| | iPP–DPM | 7.7 | 9.5 | 0.81 |
| 100 | iPP–MS | 9.7 | 13.5 | 0.72 |
| | iPP–DPE | 6.0 | 8.3 | 0.72 |
| | iPP–DPM | 5.8 | 5.9 | 0.98 |

showed the largest droplet, whereas the iPP–DPM system showed the smallest.

For droplet growth, several mechanisms such as coalescence and Ostwald ripening have been reported.[19] Recently, McGuire et al.[20] proposed a coalescence-induced coalescence mechanism. In this model, forces created as a result of a coalescence event cause a flow of the matrix fluid, which then impacts nearby droplets and causes more coalescence. They showed good quantitative agreement between the model and the experimental droplet-growth data in the iPP–DPE system. The droplet-growth rate in this mechanism is dependent on the polymer–diluent interfacial tension, increases with increasing volume fraction of the droplet phase, and decreases with increasing viscosity of the polymer-rich matrix phase.[20,21] The volume fraction of the droplet phase, interfacial tension, and viscosity of the polymer-rich matrix phase are summarized in Table II for three systems. The volume fraction of the droplet phase was obtained from the phase diagram shown in Figure 2. Heinrich and Wolf[22] measured the interfacial tension between the coexisting phases of the polystyrene/methylcyclohexane and polystyrene/cyclohexane systems. The following generalized equation, useful at least for typical vinyl polymers, was presented:

$$\sigma(\text{mN/m}) = 0.153 N_u^{0.5} \Delta\phi_2^{3.85} \quad (4)$$

where $N_u$ is the number of monomeric units and $\Delta\phi_2$ is the difference in the polymer volume fractions in the coexisting phases. As a first approximation, the interfacial tension was estimated by eq. (4) in this work. The droplet phase fractions are hardly influenced by the kind of diluents. Thus, the difference in the droplet-growth rate shown in Figure 5 cannot be explained by the difference in the droplet phase fractions. Also, for the interfacial tension, the difference by the diluents is not so pronounced. In addition, the effect of the interfacial tension on the droplet growth is less than that of the matrix phase viscosity.[20] Contrary to the previous two factors, the difference in the viscosities of the polymer-rich phase is remarkable. The viscosity in the iPP–DPM system is 4.5 times larger than that in the iPP–MS system. Therefore, the difference in the droplet-growth rates is mainly attributable to that in the matrix phase viscosity. The diluent change brings about the change of the location of the binodal line. When the binodal line is located at the higher temperature, the viscosity of the polymer-rich phase becomes lower, which leads to the higher droplet growth. This is the case in the iPP–MS system.

Figure 6 shows droplet growth under a nonisothermal condition when the polymer solution was cooled to 298 K at a constant rate of 10 or 100 K/min. The difference in the droplet sizes in the three systems was more pronounced in Figure 6(a) than in Figure 5. Arrows in Figure 6(a) indicate points where the solution temperature reached the crystallization temperature. The droplet growth almost stopped when the crystallization occurred. As the binodal line was shifted to the higher temperature, the region between the binodal line and the crystallization temperature became wider. This means the time interval for the droplet growth was longer. Thus, the largest droplet was obtained in the iPP–MS system, whereas the iPP–DPM system gave the smallest droplet. When the cooling rate was as fast as 100 K/min, the difference in the droplet sizes was not so large, as shown in Figure 6(b). This is because even in the iPP–MS system with the highest binodal line, the time interval for the droplet growth was short because of the fast cooling rate.

### Membrane Structure

Figure 7 shows cross sections of membranes prepared by cooling at 10 and 100 K/min. The tendency in the pore sizes is the same as that in the droplet size shown in Figure 6, indicating that the pore size is directly related to the droplet size. The pore size measured by SEM and the droplet size measured by optical microscopy are compared in Table III. The pore sizes were about 80% of the droplet size. A similar tendency was reported by Kim et al.[23] As they pointed out, the smaller pore size is probably due to shrinkage of the sample during the extraction of the diluent and the subsequent drying.

The membrane structures are shown in Figure 8 when the polymer solution was quenched in ice water. In all cases, interconnected structures, which are typical in the early stage of spinodal decomposition (SD), were obtained. These structures are in contrast to pore structures in Figure 7. In the L–L phase separation of a polymer solution, two different mechanisms have to be considered; nucleation and growth (NG) and SD.[24] The NG mechanism occurs in a metastable region in the phase diagram between the binodal and spinodal lines. However, SD is the expected mechanism in an unstable region inside the spinodal line. In this case, because the cooling rate was extremely high in quenching in the ice water, the phase separation occurred in the unstable region, and the structure was fixed without enough coarsening. The structure in the iPP–MS system was somewhat larger than in the iPP–DPM system. Thus, even in the rapid quenching process, a diluent effect on the membrane structure appeared. The larger structure in the iPP–MS system may be due to the longer time for the structure growth brought about by the wider region between the binodal line and the crystallization temperature.

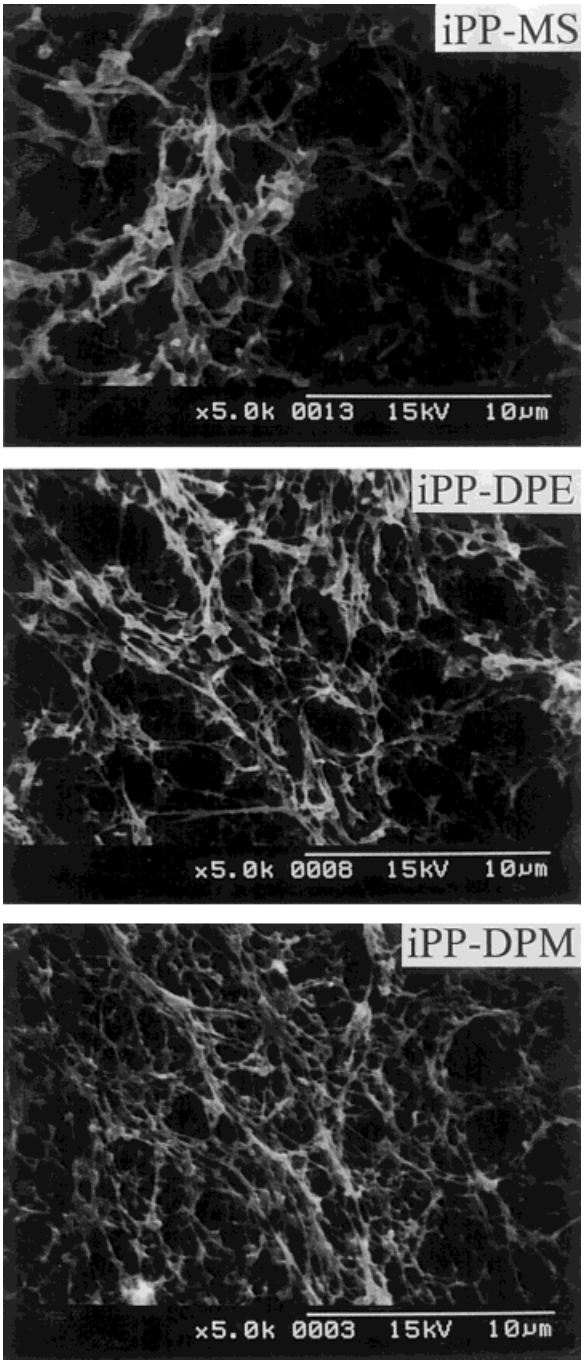


**Figure 8** Membrane structures for a polymer solution quenched into ice water with a polymer concentration of 10 wt %.

## CONCLUSION

1. Phase diagrams were obtained for three iPP–diluent systems. The cloud-point curve was shifted to the lower temperature in the order iPP–MS, iPP–DPE, and iPP–DPM. This order can be explained by the compatibility between iPP and diluents. The crystallization temperature was not influenced so much by the diluent type.
2. The droplet-growth process was followed by optical microscopy. When the polymer solution was quenched and the temperature was maintained at a constant value, the droplet-growth rate decreased in the order iPP–MS, iPP–DPE and iPP–DPM. The main reason for this tendency was the difference in the matrix phase viscosity.

When the solution was cooled at a constant cooling rate, the difference in the droplet sizes in three systems was pronounced. This was attributable to the difference in the time interval for the droplet growth.

3. Under the condition of a constant cooling rate, the pore size measured by SEM was directly related to the droplet size by optical microscopy, whereas the former was larger than the latter. When the polymer solution was quenched in the ice water, interconnected structures were obtained. The structure in the iPP–MS system was somewhat larger than in the iPP–DPM system.

## REFERENCES


1. Castro, A. J. U.S. Pat. 4,247,498 (1981).
2. Caneba, G. T.; Soong, D. S. Macromolecules 1985, 18, 2538.
3. Hiatt, W. C.; Vitzthum, G. H.; Wagener, K. B.; Gerlach, K.; Josefiak, C. In Microporous Membranes via Upper Critical Temperature Phase Separation; Lloyd, D. R., Ed.; ACS Symposium Series 269; American Chemical Society: Washington, DC, 1985; p 229.
4. Aubert, J. H.; Clough, R. L. Polymer 1985, 26, 2047.
5. Lloyd, D. R.; Kinzer, K. E.; Tseng, H. S. J Membr Sci 1990, 52, 239.
6. Tai, F.-J.; Torkelson, J. M. Macromolecules 1990, 23, 775.
7. Lloyd, D. R.; Kim, S. S.; Kinzer, K. E. J Membr Sci 1991, 64, 1.
8. Kim, S. S.; Lloyd, D. R. J Membr Sci 1991, 64, 13.
9. Vandeweerdt, P.; Berghmans, H.; Tervoort, Y. Macromolecules 1991, 24, 3547.
10. Berghmans, S.; Mewis, J.; Berghmans, H.; Meijer, H. E. H. Polymer 1995, 36, 3085.
11. Caplan, M. R.; Chiang, C. Y.; Lloyd, D. R.; Yen, L. Y. J Membr Sci 1997, 130, 219.
12. Lee, H. K.; Myerson, A. S.; Levon, K. Macromolecules 1992, 25, 4002.
13. Vadalia, H. C.; Lee, H. K.; Myerson, A. S.; Levon, K. J Membr Sci 1994, 89, 37.
14. Nabetani, H. In Viscosity (in Japanese); Kimura, S.; Nakao, S.; Ohya, H.; Nakagawa, T., Eds.; Kyoritsu Shuppan: Tokyo, 1993; p 210
15. Polymer Handbook, 3rd ed.; Brandrup, J.; Immergut, E. H., Eds.; Wiley: New York, 1989.
16. Barton, A. F. M. Handbook of Solubility Parameters and Other Cohesion Parameters, 2nd ed.; CRC: Boca Raton, FL, 1991.
17. Flory, P. J. Principles of Polymer Chemistry; Cornell University Press: Ithaca, 1953.
18. McGuire, K. S.; Laxminarayan, A.; Lloyd, D. R. Polymer 1994, 35, 4404.
19. Siggia, E. D. Phys Rev A 1979, 20, 595.
20. McGuire, K. S.; Laxminarayan, A.; Martula, S.; Lloyd, D. R. J Colloid Interface Sci 1996, 182, 46.
21. McGuire, K. S.; Laxminarayan, A.; Lloyd, D. R. Polymer 1995, 36, 4951.
22. Heinrich, M.; Wolf, B. A. Polymer 1992, 33, 1926.
23. Kim, S. S.; Yeom, M.-O.; Cho, I.-S. In Thermally-Induced Phase Separation Mechanism Study for Membrane Formation; Pinnau, I.; Freeman, B. D., Eds.; ACS Symposium Series 744; American Chemical Society: Washington, DC, 1999; p 42.
24. Van de Witte, P.; Dijkstra, P. J.; van den Berg, J. W. A.; Feijen, J. J Membr Sci 1996, 117, 1.